ChemPubSoc Europe

DOI: 10.1002/cplu.201700296

CHEMPLUSCHEM Full Papers

Real-Time Reaction Monitoring of an Organic Multistep Reaction by Electrospray Ionization-Ion Mobility Spectrometry

Martin Zühlke, Stephan Sass, Daniel Riebe, Toralf Beitz, and Hans-Gerd Löhmannsröben*[a]

The capability of electrospray ionization (ESI)-ion mobility (IM) spectrometry for reaction monitoring is assessed both as a stand-alone real-time technique and in combination with HPLC. A three-step chemical reaction, consisting of a Williamson ether synthesis followed by a hydrogenation and an *N*-alkylation step, is chosen for demonstration. Intermediates and products are determined with a drift time to mass-per-charge correlation. Addition of an HPLC column to the setup increases the separation power and allows the determination of further species. Monitoring of the intensities of the various species over the reaction time allows the detection of the end of reaction, determination of the rate-limiting step, observation of the system response in discontinuous processes, and optimization of the mass ratios of the starting materials. However, charge competition in ESI influences the quantitative detection of substances in the reaction mixture. Therefore, two different methods are investigated, which allow the quantification and investigation of reaction kinetics. The first method is based on the pre-separation of the compounds on an HPLC column and their subsequent individual detection in the ESI-IM spectrometer. The second method involves an extended calibration procedure, which considers charge competition effects and facilitates nearly real-time quantification.

Introduction

A deeper understanding of chemical reactions is an essential requirement for optimizations of chemical synthesis in research and industry. Fast online detection methods enable the determination of reactive intermediates and the rate-limiting step, and consequently, allow the elucidation of the reaction kinetics and the underlying reaction mechanism. Typical techniques for monitoring reactions are spectroscopic methods such as near-infrared (NIR),[1] ultraviolet (UV),[2] Raman,[3] or nuclear magnetic resonance (NMR) spectroscopy,[4] which often allow direct contactless access to the reaction mixture, avoiding any disturbance and providing real-time monitoring. A number of different syntheses can be monitored spectroscopically. Nevertheless, various properties can hamper applications, such as low sensitivity for dilute intermediates (Raman), high complexity of the reaction mixture (UV, NIR, Raman), or difficult interpretation of spectra or impurities (NMR). Other techniques such as mass spectrometry (MS)[5,6] and chromatographic methods[7] allow the characterization of more complex reactions. Gas chromatography (GC) and liquid chromatography (LC) are proven techniques for synthesis control in the industry, but are often time-consuming. In the case of MS, many publications demonstrate the fast analysis of the compounds in the reaction. However, expensive equipment and, in the case of atmospheric pressure ionization (API) sources, charge competition influencing the ionization efficiency of the individual components are disadvantageous.

A technique less often applied in reaction monitoring is ion mobility (IM) spectrometry, which is less expensive than MS. The fundamental principle of IM spectrometry is the separation of ions according to their mobility (K) in an electric field (E), usually at atmospheric pressure. The mobility K is a characteristic physical constant for a molecular ion in a drift gas, and is described by the Mason equation, shown in Equation (1).[8]

$$K = \frac{l}{Et_D} = \frac{3}{16}\frac{q}{N}\left(\frac{1}{m}+\frac{1}{M}\right)^{1/2}\left(\frac{2\pi}{k_B T_{eff}}\right)^{1/2}\frac{1}{\Omega_D} \quad (1)$$

Here, l is the drift path length, t_D is the drift time, q is the charge, N is the number density of the drift gas, m is the mass of the drift gas molecules, M is the mass of the ions, T_{eff} is the temperature in the drift tube, k_B is the Boltzmann constant, and Ω_D is the collisional cross section. Ω_D is a measure of the shape of an ion, and is the most important parameter in IM spectrometry. In contrast to MS, in IM spectrometry, the collisional cross section determines the separation, and thus, isomers can be separated. The ionization methods most frequently applied in IM spectrometry are either based on the evaporation of analytes with subsequent ionization in the gas phase by chemical ionization at atmospheric pressure (APCI) through electron- or proton-transfer reactions (e.g., with ^{63}Ni or corona discharge), or rely on the direct ionization of liquids by electro-

[a] M. Zühlke, S. Sass, D. Riebe, T. Beitz, Prof. Dr. H.-G. Löhmannsröben
University of Potsdam, Physical Chemistry
Karl-Liebknecht-Strasse 24–25
14476 Potsdam–Golm (Germany)
E-mail: loehm@uni-potsdam.de
Homepage: http://www.chem.uni-potsdam.de/groups/pc

Supporting information for this article can be found under: https://doi.org/10.1002/cplu.201700296.

spray ionization (ESI) or matrix-assisted laser desorption/ionization (MALDI).[9]

Only a few applications of APCI-IM spectrometry for reaction monitoring have been reported. These include the online monitoring of monomer concentrations (vinyl acetate) in (semi-) batch emulsion polymerization reactors,[10] and a kinetic study of the acetylcholine hydrolysis catalyzed by acetylcholinesterase (AChE) and its inhibition by neostigmine and galanthamine.[11] In 2010, the company Excellims demonstrated reaction monitoring of the Michael addition of cyclohexylethylamine to dimethlitaconate using ESI-IM spectrometry.[12] Several studies have focused on the potential of ESI-IM in combination with mass spectrometry (IM-MS) for reaction monitoring. In one study,[13] the monitoring of the reaction products formed upon deprotonation of 7-fluoro-6-hydroxy-2-methylindole by aqueous sodium hydroxide was investigated, demonstrating the advantages of the IM-MS method combination. Other studies have shown the detection of short-lived intermediates and quantitative investigations monitoring the reductive amination reaction of nicotinaldehyde and 4-picolylamine to di-(2-picolyl)-amine.[14] In another study, the combination of stable isotope labelling with direct infusion IM-MS was investigated for qualitative and quantitative monitoring of biocatalytic reactions.[15] This approach was applied to lipase and monooxygenase enzymes and included multisubstrate screening.

However, for the less expensive, stand-alone ESI-IM spectrometry, a demonstration of the quantitative monitoring of all the components of a reaction mixture is still lacking. Herein, the capability of ESI-IM spectrometry was evaluated, both as a stand-alone method and in combination with HPLC, for qualitative and quantitative reaction monitoring. The enhancement of the separation power through the combination of HPLC with ESI-IM spectrometry is based on our previous work.[16,17] A three-step reaction consisting of a Williamson ether synthesis followed by a hydrogenation and an *N*-alkylation reaction was chosen for the characterization of reaction monitoring by ESI-IM spectrometry. These reaction steps are used frequently in chemical syntheses. The ether synthesis and the alkylation are representative of classical electrophilic or nucleophilic substitutions, whereas the hydrogenation is an example of heterogeneous catalysis. However, the product is BAPTA-AM, which is a precursor of the calcium sensor BAPTA, which is used for spectroscopic in vivo measurements in biological applications.[18,19]

Results and Discussion

In this study, all three steps of the reaction sequence (Figure 1) were monitored over the whole reaction time. Each reaction step was performed separately in a flask. The reaction conditions of each step were based on literature-known syntheses.[20–23] The detailed conditions can be found in the Supporting Information (S.1.2 Synthesis). Each step was followed by a work-up, and the purified products were analyzed by standard analytical methods before their utilization as the starting materials for the respective next step. At different reaction times, samples were taken by syringe and introduced into the ESI-IM spectrometer (see Experimental Section for details). This section is divided into three parts, which are focused on the determination of reaction intermediates and products, on different tasks of reaction monitoring based on the pure intensities, and on two methods allowing the quantification of all components in the reaction mixture. In these sections, ESI-IM spectrometry is characterized as a stand-alone technique as well as in combination with HPLC for pre-separation. In each section, only one reaction step is discussed for demonstration purposes.

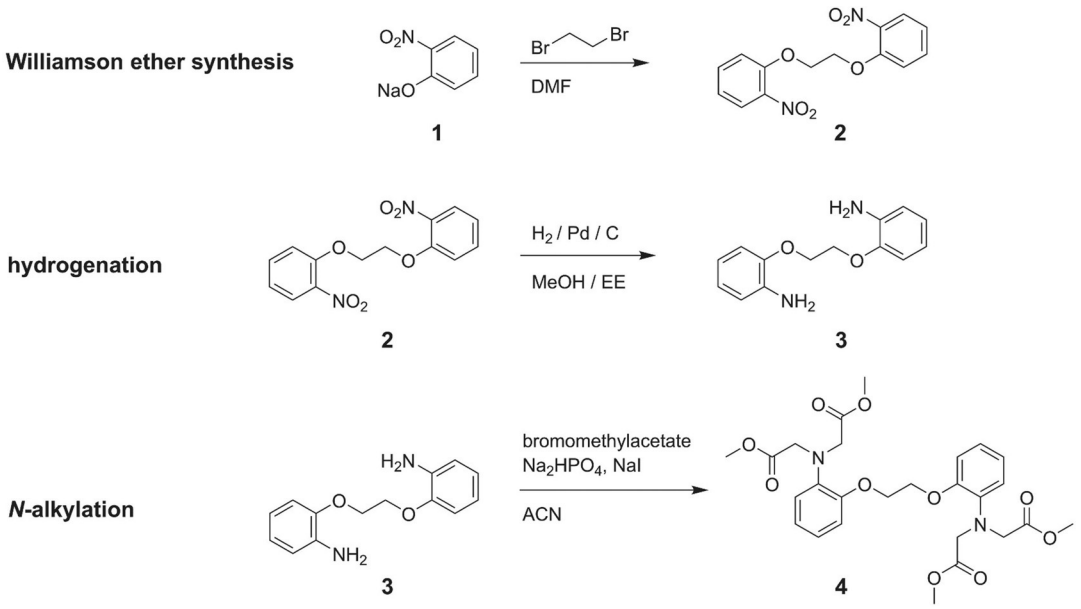

Figure 1. Reaction sequence starting from 1,2-dibromoethane and sodium 2-nitrophenoxide to 1,2-bis(aminophenoxy)ethane-*N*,*N*,*N*′,*N*′-tetraacetic acid methylester (BAPTA-AM).

Intermediate and product detection

Direct detection by IM spectrometry

ESI-IM spectrometry enables the very fast detection of intermediates and products. For demonstration purposes, the *N*-alkylation of substance **3** to **4**, which constitutes the most complex reaction step and includes the highest number of intermediates, was chosen. Figure 2a shows three IM spectra taken after reaction times of 3, 25, and 390 min. In the IM spectra, the discharge current (intensity in nA) of all ions arriving the detector at the same drift time is plotted over their drift time (drift time in ms). The peak group at 5–7 ms observed in all IM spectra is attributed to solvent cluster ions. The five peaks at 9–15 ms can be assigned to the starting material, different intermediates, and the product. They have a constant peak-to-peak distance (Δt_D) of approximately 1.13 ms, indicating a structural relation as well as a constant mass difference between neighboring peaks. In the IM spectrometry literature, there are several examples of substances belonging to homologous series showing good correlations between drift time (or inverse ion mobility) and mass, facilitating simple mass assignments of unknown members of the series.[24] Assuming singly protonated molecules (M + 1) for the five peaks between 9 and 15 ms, as are usually observed for small molecules in ESI, the drift times of the corresponding ions can be plotted against the mass-to-charge ratio (*m/z*) to verify the species. The high correlation of the detected constituents shown in Figure 2b possesses a coefficient of determination of $R^2 = 0.99$ and allows reliable assignment of the IM peaks to constituents of the reaction mixture. The starting material has the lowest drift time. Increasing degrees of *N*-alkylation lead to a peak shift to higher drift times. Thus, the peak with the highest drift time can be assigned to the product, and the intermediates to the one-, two-, and three-times substituted species of the starting material **3**. The assumed M + 1 peak for the starting material and product was verified through MS measurements (see Supporting Information). In contrast to HPLC separation (Figure 3), which shows a less clear order of substance peaks, in IM spectrometry, the analytes are ordered by size.

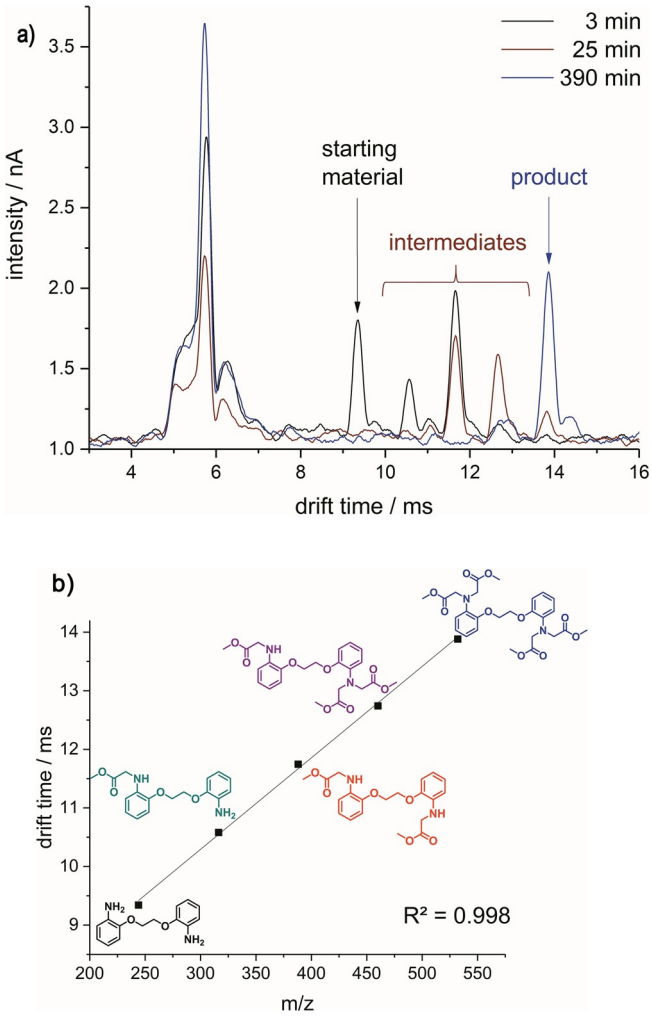

Figure 2. Consecutive *N*-alkylation of subtance **3** to **4**. a) IM spectra at different reaction times (drift time 5–7 ms for the solvent cluster peak, and 9–14 ms for the five different species of the *N*-alkylation). b) Direct determination of the five species of the *N*-alkylation from drift time versus mass-to-charge ratio (*m/z*).

There is an alternative, more elaborate method of peak assignment based on the quantum chemical calculation of substance structures and the subsequent determination of collision cross sections by programs calculating collision trajectories.[25–27] Mobilities can be obtained from the cross sections by the Mason equation [Eq. (1)]. The cost of calculation increases in the case of flexible molecules, for which all energy-averaged conformations must be considered by applying molecular dynamics simulations.

Two-dimensional detection by HPLC-IM spectrometry

The peak capacity *n* in IM spectrometry is often limited to $n < 10$. Thus, the combination of IM spectrometry with a separation method of high orthogonality, for example, HPLC, can facilitate the complete separation of complex reaction mixtures. New information can appear owing to the complementary separation on the LC column and in the drift tube. Because of the different time scales of HPLC (minutes) and IM spectrometry (milliseconds), both methods can be combined easily, yielding 2D spectra consisting of the dimensions of retention and drift time.[16,17] A 2D spectrum of the consecutive *N*-alkylation from **3** to **4** is shown in Figure 3 at the reaction time corresponding to the maximum intensity of the disubstituted species (5 min). All constituents of the reaction mixture can be separated in the plane of the 2D spectrum. The species can also be determined from the drift time versus *m/z* ratio, as in the 1D IM spectrum. In comparison with the 1D IM spectrum, additional compounds are found. In addition to the five species observed in the IM spectra (Figure 2a), the disubstituted species peak is split into two different peaks, which can be assigned to two constitutional isomers. The *N*,*N*-disubstituted species has the two alkyl chains on the same nitrogen atom. In the *N*,*N*′-disubstituted species, each nitrogen atom is connected to an alkyl chain. The *N*,*N*-disubstituted species elutes first because of its higher polarity. Computational calculations using density functional theory (DFT) show that the charge density at the nitro-

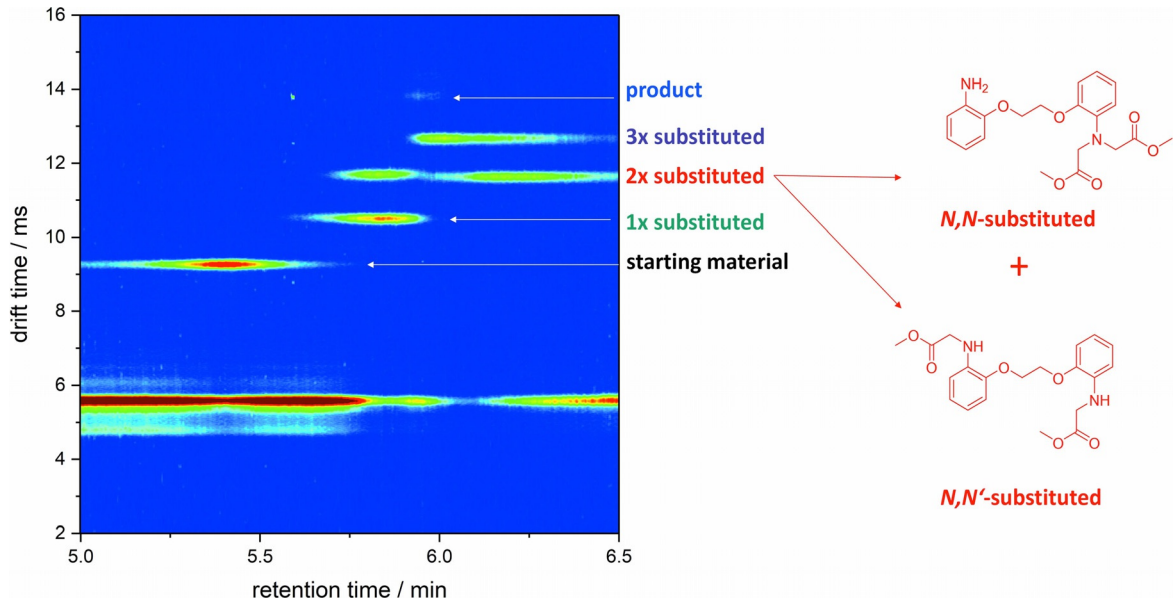

Figure 3. Consecutive *N*-alkylation of subtance **3** to **4**. HPLC ESI-IMS spectrum at 5 min reaction time (the colors of the words refer to Figure 2b for color code of the subtances; drift time 5–7 ms for solvent cluster peak and 9–14 ms for the five different species of the *N*-alkylation).

gen atom decreases with increasing substitution owing to the electron-withdrawing effect of the carbonyl group. This correlates with approximations of the pK_a value, which decreases at higher substitution.[28] The area of the first peak is only half that of the second peak. This suggests that the *N*,*N*′-substitution is preferred. This experimental result is in agreement with quantum chemical calculations on the reaction pathway. The three-step calculation procedure starts with a systematic variation of the torsion angle in AMBER, followed by PM7 and B3LYP/6-31G(d)+D3 optimizations (see Supporting Information, S.3). The energy calculated for the ground-state conformation of the *N*,*N*′-substituted species is 33 kJ mol^{-1} below that of the corresponding *N*,*N*-isomer. This difference could explain the preferred formation. The separation on the reversed-phase LC column is poor. The effect of the increasing mass gained with each additional *N*-alkylation step is cancelled by the increasing polarity of the alkylated amine caused by the carbonyl groups.

Process monitoring

In certain process monitoring tasks, exact knowledge of the concentrations is not always required; tracking of relative intensities can provide the necessary information. These tasks include the detection of the end of reaction, determination of the rate-limiting step, observation of the system response in discontinuous processes, and optimization of the mass ratio of the starting materials.

Direct monitoring by IM spectrometry

After the qualitative determination of the components in the reaction mixture, their temporal appearance profile is interesting because it allows the determination of the rate-limiting step and the deduction of the reaction mechanism. As IM spectra can be measured in less than one second, IM spectrometry enables the measurement of a large number of samples in a short time, and thus, allows almost real-time monitoring (sampling is the limiting factor). The reaction progress of the *N*-alkylation was monitored over 24 h and is presented in Figure 4. The normalized intensities of all five *N*-alkylation species over the reaction time are displayed, enabling a conversion control. The intensity maxima of all components are passed sequentially. Furthermore, the time between subsequent intensity maxima increases, which indicates a decrease in the rate constants of each additional alkylation step. The rate-limiting step is the last alkylation step; one reason for this could be the steric hindrance of the three alkyl chains, impeding this final alkylation.

A well-known problem in ESI is charge competition between analytes, which can lead to their partial or complete suppression. As already discussed, the negative charge density at the nitrogen decreases with each alkylation step. This is reflected in the pK_a values, which also decrease with each alkylation step. Hence, it is probable that the intensity curves are influenced by charge competition.[29] Therefore, HPLC-IM spectrometry measurements (not shown) were taken to address this issue. Although the intermediates could not be separated completely in the LC dimension, the curves of the educt, intermediates, and product in Figure 4 could be reproduced qualitatively, indicating that the influence of the charge competition effect is not strong.

Monitoring by HPLC-IM spectrometry

The focus of the previous subsection was the detection of the end of reaction and the determination of the rate-limiting step. In this part, a discontinuous process is simulated, allow-

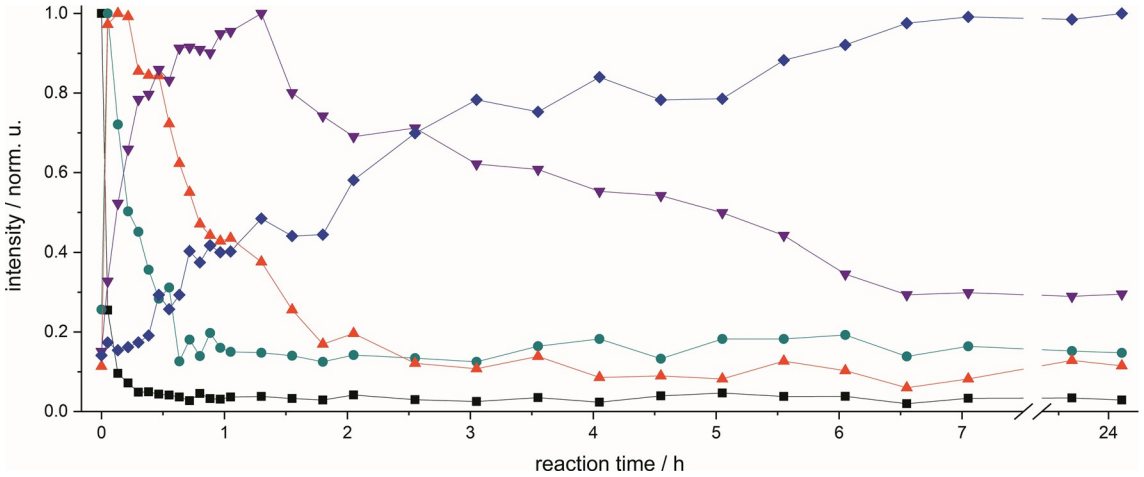

Figure 4. Consecutive *N*-alkylation of subtance **3** to **4** over the reaction time (refer to Figure 2b for the color code: starting material **3** (black), 1×substituted species of **3** (cyan), 2×substituted species of **3** (red), 3×substituted species of **3** (purple), product **4** (dark blue); intensities were normalized separately).

ing observation of the system response and optimization of the mass ratio of the starting materials. In comparison with the *N*-alkylation, charge competition is much stronger among the species involved in the Williamson ether synthesis. Therefore, HPLC-IM spectrometry was used for reaction monitoring.

The discontinuous process is simulated by stepwise injection of the starting material **1**, changing the molar ratio between the starting materials from 1:1 to 3:1. The intensities of the starting material **1** (black), the intermediate (green), and the product **2** (blue) were monitored (Figure 5). After each injection, the concentration of the starting material rises immediately before it declines, and after a short initial period, the product concentration increases before reaching a plateau. The temporal concentration profile of the intermediate is more interesting. The reaction pathway shown at the top of Figure 5 indicates that the starting material **1** first reacts with 1,2-dibromoethane to form the intermediate. Then, the intermediate reacts with **1** again to produce **2**. Therefore, for the formation of product **2**, 1 mol of 1,2-dibromoethane and 2 mol of **1** are needed. Because of the initial molar ratio (1:1), the intermediate is formed as the main product. After the second injection, a strong increase in the concentration of the intermediate is observed, caused by the reaction of **1** with the remaining 1,2-dibromoethane. Subsequently, the intermediate reacts to form

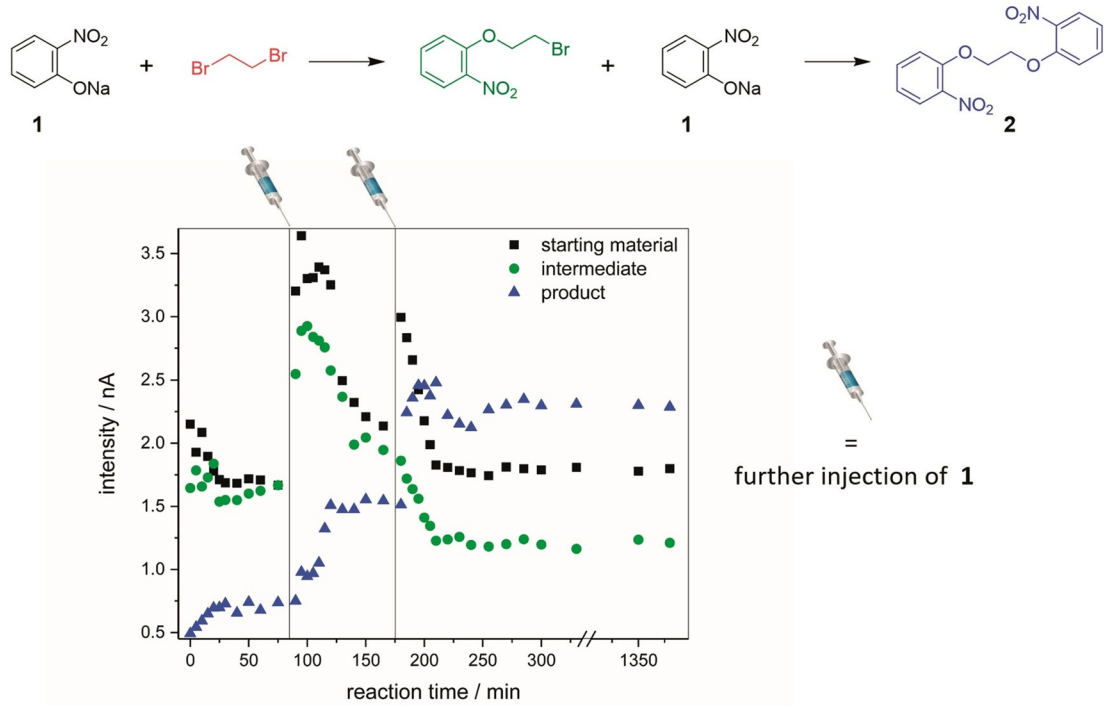

Figure 5. Intensity over reaction time of the Williamson ether synthesis for starting material **1**, intermediate, and product **2**, with a stepwise injection of starting material **1**.

the product because of the optimal molar ratio between the starting materials. After the third injection, the intensity of the intermediate does not increase further owing to the surplus of starting material **1**. Thus, the ratio of both starting materials, **1** and 1,2-dibromoethane, determines the reaction yield and the concentration level of the intermediate.

Quantification

Charge competition influences the quantitative detection of all compounds in the reaction mixture, so two different methods were investigated, which consider this effect and allow the quantitative determination of all substances. The first method is based on the pre-separation of the compounds on an HPLC column and their subsequent individual detection in the ESI-IM spectrometer. The second method involves an extended calibration procedure that takes charge competition effects into account. The benefit of this method is the nearly real-time quantification by direct IM spectrometry without the need for a pre-separation step. For the illustration of both methods, the hydrogenation was chosen as an example of a heterogeneous reaction.

HPLC-IM spectrometry: quantification, kinetics, and conversion control

The separate calibrations of the isolated starting material **2** and product **3** show a linear range of around two orders of magnitude (Figure 6a). From this calibration and the pre-separation of all constituents of the reaction mixture, concentration–time profiles over the complete reaction time were determined (Figure 6b). There are three notable features in these profiles. The first is the fast drop of the concentration of **2** owing to adsorption on the activated carbon (catalyst), which is not sampled. The second feature is the linear decrease in the concentration of the starting material after this initial period of adsorption, and the linear increase in the product concentration with reaction time. After 90 min, **2** and **3** reach a plateau, signifying the final conversion of the reaction. Fitting of the linear segment yields good coefficients of determination ($R^2 = 0.86$ for **2**, $R^2 = 0.97$ for **3**). This allows the determination of rate constants and indicates a reaction order of zero. The zero-order rate constant obtained for the decrease in starting material is $k_2 = (2.1 \pm 0.2)\ \mu mol\, s^{-1} L^{-1}$, and that for the formation of the product is $k_3 = (2.2 \pm 0.1)\ \mu mol\, s^{-1} L^{-1}$. These rate constants have similar values, indicating that side reactions do not occur.

IM spectrometry: direct quantification

The quantification without pre-separation on an HPLC column requires an extended calibration procedure, which considers charge competition effects. In addition to the normal calibration procedure of the individual substances, the mutual suppression of starting material and product must be considered. One possible method is the calculation of concentration-dependent correction factors. The correction factors are based on

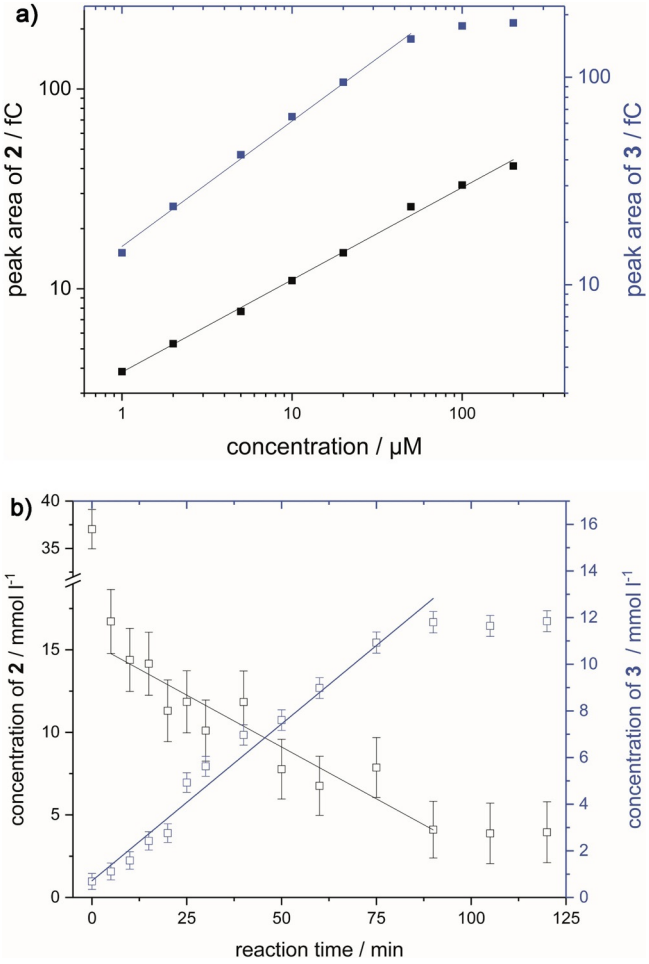

Figure 6. Reaction monitoring of the hydrogenation of **2** (black traces) yielding **3** (blue traces) with HPLC ESI-IM spectrometry: a) calibration, and b) concentration over reaction time.

the fact that there are a limited number of charges in a droplet produced during the ESI process.[30] If there is only one ionizable compound in the droplet, all charges are available to it. If there is more than one ionizable compound, all compounds compete for the same pool of charges. Assuming that the overall number of ions produced by ESI is nearly constant, the sum area of all IM peaks should be nearly constant as well (neglecting diffusion processes). The following procedure for the calculation of the correction factors was applied: IM spectra were measured using a constant concentration of **2** and a varying concentration of **3**, and vice versa. In the absence of **3**, the peak intensity of **2** is at its maximum. Increasing concentrations of **3** lead to a decrease in the peak intensity of **2**. The maximum peak intensity of **2** divided by the peak intensity of **2** at a defined concentration of **3** yields an individual correction factor. The correction factor (CF) depends on the relative intensities of both compounds. Hence, for every intensity ratio of **2** and **3**, there is a CF for each compound. The relationship for **2** is displayed in Figure 7a, and can be described by an asymptotic function. Nonlinear regression gives the following function parameters: $CF = 0.89 - 1.07 \times 0.98^x$ and $R^2 = 0.995$. Here, x describes the ratio of the intensities of starting material

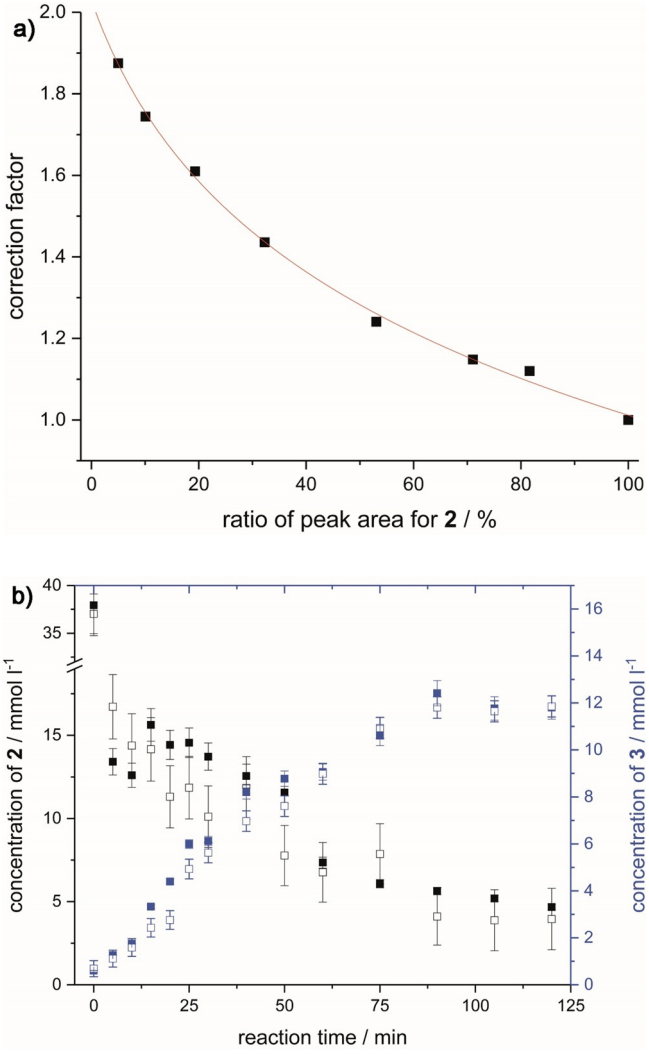

Figure 7. Reaction monitoring of the hydrogenation with ESI-IM spectrometry: a) correction factor of **2** for charge competition as a function of the ratio of intensities of **2** and **3**, b) concentrations of **2** (black) and **3** (blue) over reaction time in direct ESI-IM spectrometry (filled symbols) versus HPLC-ESI-IM spectrometry (open symbols).

2 and product **3**. The correction function was applied to the peak intensities, yielding concentrations. The temporal concentration profiles obtained by both methods, that is, HPLC-IM spectrometry and direct IM spectrometry with the extended calibration procedure, are compared in Figure 7b.

Both methods yield similar results. However, this finding might only apply to this specific case, as the range of concentrations investigated is relatively narrow. For a more general approach, the correction factor vector used here should be extended to a correction matrix that takes into account additional constant concentrations of **2** at varying concentrations of **3** (and vice versa).

Conclusion

This study demonstrates that ESI-IM spectrometry can be applied for reaction monitoring. A three-step reaction sequence consisting of a Williamson ether synthesis followed by a hydrogenation and an *N*-alkylation step were investigated. On the one hand, IM spectrometry can be used as a stand-alone method for qualitative and quantitative real-time monitoring of reaction mixtures of low complexity. On the other hand, the inclusion of a pre-separation step through HPLC enables the investigation of more complex mixtures, albeit at the expense of the real-time ability. IM spectrometry was shown to allow the determination of all reaction participants including intermediates, relative-intensity-based (without calibration) monitoring, and concentration-based (with calibration) monitoring of the reaction process.

The determination of the various compounds is based on their ion mobilities, which are characteristic physical constants for any ion-drift gas molecule pair. A reliable assignment of substances on the basis of their measured mobilities can require demanding DFT calculations. However, simple drift time–mass correlations of the reactants are often sufficient, but IM resolutions are often limited to 60 results in overlapping peaks in the IM spectrum.[31] If the composition of the reaction mixture is too complex for stand-alone IM spectrometry, 2D LC-IM spectrometry can enable the separation of all substances. Such separation benefits from the high orthogonality of the different separation principles.[16]

Relative-intensity-based measurements can yield valuable information, but avoid extensive calibration. This could be shown for the detection of the end of reaction, the determination of the rate-limiting step, the observation of the system response in discontinuous processes, and the optimization of the mass ratio of the starting material components. Charge competition in the ESI process can influence the measured intensities; complete suppression of some substances is possible. Therefore, 2D HPLC-IM spectrometric separations should be performed for evaluation of these charge competition effects.

If the charge competition effects cannot be neglected, LC-IM spectrometric separation in combination with calibration yields concentration information on the reaction process. An alternative, allowing almost real-time measurements, involves the application of an extended calibration procedure. Although this procedure usually requires a large number of measurements, the simplified version applied in this study can give satisfactory results.

Experimental Section

All IM spectra were recorded with a home-built ESI-IM spectrometer, which has been described in detail previously.[17] The spectrometer is divided into four sections. The first part is the cylindrical ionization region (inner diameter, ID = 30 mm) containing an ESI capillary (Hamilton, gauge 32) inserted into a 1/16" steel capillary arranged orthogonally to the axis of the IM spectrometer. This region is followed by a desolvation (length = 50 mm, outer diameter, OD = 47.5 mm, ID = 25 mm, thickness = 23 mm, repeating unit = 3.17 mm, T = 160 °C) and a drift region (length = 100 mm, OD = 47,5 mm, ID = 25 mm, thickness = 2.54 mm, repeating unit = 3.17 mm, T = 140 °C) separated by an ion gate in the Bradbury–Nielsen design. The fourth part is the detection region consisting of a Faraday plate with a diameter of 18 mm connected to a 10^9 V/A amplifier (Physimetron A6203) and an oscilloscope (Handyscope

HS3, Tiepie). Nitrogen 5.0 (Praxair) was used as drift gas (flow rate = 1.3 L min^{-1}) and the sheath gas (flow rate = 1.8 L min^{-1}).

The HPLC system for the pre-separation of the reaction mixture consisted of an LPG pump (Azura P 6.1L, KNAUER), an injection valve (KNAUER), and a reversed-phase (RP) column (Hypersil Gold, Thermo, 100 × 2.1 mm, 3 μm). The mobile phase of all reaction mixture separations was composed of acetonitrile (solvent A) and 0.1% aqueous formic acid (solvent B), and the flow rate was 300 μL min^{-1}. Different solvent gradients were used for the following reaction mixtures:

1. Consecutive alkylation: 0–3 min, 30% A; 3–4 min, 30–90% A; 4–7 min, 90% A.
2. Alkylation: 0–1 min, 30% A; 1–2 min, 30–90% A; 2–5 min, 90% A.
3. Hydrogenation: 0–3 min, 30% A; 3–4 min, 30–90% A; 4–7 min, 90% A.

Acknowledgements

We gratefully acknowledge the financial support for this research received from the German Federal Ministry for Economic Affairs and Energy (BMWi) through the AiF (Grant No. KF2167703NT2) and Rainer Neumann for the quantum-chemical calculations. Experimental work was supported by Stefan Mies.

Conflict of interest

The authors declare no conflict of interest.

Keywords: electrospray ionization · HPLC · ion mobility spectrometry · reaction mechanisms · reaction monitoring

[1] N. Heigl, C. Petter, M. Rainer, M. Najam-ul-Haq, R. Vallant, R. Bakry, G. Bonn, C. Huck, *J. Near Infrared Spectrosc.* **2007**, *15*, 269–282.
[2] K. Grabow, U. Bentrup, *ACS Catal.* **2014**, *4*, 2153–2164.
[3] K. A. Esmonde-White, M. Cuellar, C. Uerpmann, B. Lenain, I. R. Lewis, *Anal. Bioanal. Chem.* **2017**, *409*, 637–649.
[4] F. Dalitz, M. Cudaj, M. Maiwald, G. Guthausen, *Prog. Nucl. Magn. Reson. Spectrosc.* **2012**, *60*, 52–70.
[5] L. S. Santos, *Reactive Intermediates: MS Investigations in Solution*, Wiley-VCH, Weinheim, **2009**.
[6] D. Schröder, *Acc. Chem. Res.* **2012**, *45*, 1521–1532.
[7] W. A. Schafer, S. Hobbs, J. Rehm, D. A. Rakestraw, C. Orella, M. McLaughlin, Z. Ge, C. J. Welch, *Org. Process Res. Dev.* **2007**, *11*, 870–876.
[8] E. A. Mason, E. W. McDaniel, *Transport Properties of Ions in Gases*, John Wiley & Sons, Weinheim, FRG, **1988**.
[9] H. Borsdorf, T. Mayer, M. Zarejousheghani, G. A. Eiceman, *Appl. Spectrosc. Rev.* **2011**, *46*, 472–521.
[10] W. Vautz, W. Mauntz, S. Engell, J. I. Baumbach, *Macromol. React. Eng.* **2009**, *3*, 85–90.
[11] S. Armenta, M. Blanco, *Anal. Chim. Acta* **2011**, *685*, 1–8.
[12] C. Krueger, C. Hilton, M. Osgood, J. Wu, C. Wu, Appl. Note IMS-2010-01A, **2010**, 1–4.
[13] E. L. Harry, A. W. T. Bristow, I. D. Wilson, C. S. Creaser, *Analyst* **2011**, *136*, 1728–1732.
[14] K. M. Roscioli, X. Zhang, S. X. Li, G. H. Goetz, G. Cheng, Z. Zhang, W. F. Siems, H. H. Hill, Jr., *Int. J. Mass Spectrom.* **2013**, *336*, 27–36.
[15] C. Yan, J. W. Schmidberger, F. Parmeggiani, S. A. Hussain, N. J. Turner, S. L. Flitsch, P. Barran, *Analyst* **2016**, *141*, 2351–2355.
[16] M. Zühlke, D. Riebe, T. Beitz, H.-G. H.-G. Löhmannsröben, S. Andreotti, K. Reinert, K. Zenichowski, M. Diener, *J. Sep. Sci.* **2016**, *39*, 4756–4764.
[17] M. Zühlke, D. Riebe, T. Beitz, H.-G. Löhmannsröben, K. Zenichowski, M. Diener, M. W. Linscheid, *Eur. J. Mass Spectrom.* **2015**, *21*, 391–402.
[18] R. Pethig, M. Kuhn, R. Payne, E. Adler, T. H. Chen, L. F. Jaffe, *Cell Calcium* **1989**, *10*, 491–8.
[19] K. Jahn, C. Hille, *PLoS One* **2014**, *9*, e105334.
[20] S. Heilporn, F. Broeders, D. Daloze, J. C. Braekman, J. M. Boeynaems, *Bull. Soc. Chim. Belg.* **1994**, *103*, 309–319.
[21] R. Y. Tsien, *Biochemistry* **1980**, *19*, 2396–2404.
[22] Y. M. A. Naguib, *Molecules* **2009**, *14*, 3600–3609.
[23] G. Grynkiewicz, M. Poenie, R. Y. Tsien, *J. Biol. Chem.* **1985**, *260*, 3440–3450.
[24] H. Borsdorf, H. Schelhorn, J. Flachowsky, H.-R. Döring, J. Stach, *Anal. Chim. Acta* **2000**, *403*, 235–242.
[25] M. F. Mesleh, J. M. Hunter, A. A. Shvartsburg, G. C. Schatz, M. F. Jarrold, *J. Phys. Chem.* **1996**, *100*, 16082–16086.
[26] A. A. Shvartsburg, M. F. Jarrold, *Chem. Phys. Lett.* **1996**, *261*, 86–91.
[27] I. Campuzano, M. F. Bush, C. V. Robinson, C. Beaumont, K. Richardson, H. Kim, H. I. Kim, *Anal. Chem.* **2012**, *84*, 1026–1033.
[28] A. C. Lee, G. M. Crippen, *J. Chem. Inf. Model.* **2009**, *49*, 2013–2033.
[29] L. W. Beegle, I. Kanik, L. Matz, H. H. Hill, Jr., *Anal. Chem.* **2001**, *73*, 3028–34.
[30] G. S. Jackson, C. G. Enke, *Anal. Chem.* **1999**, *71*, 3777–3784.
[31] K. Cottingham, *Anal. Chem.* **2003**, *75*, 435A–439A.

Manuscript received: July 4, 2017
Revised manuscript received: August 18, 2017